

Received April 14, 2020, accepted May 8, 2020, date of publication May 19, 2020, date of current version June 8, 2020.

Digital Object Identifier 10.1109/ACCESS.2020.2995647

Restoration of Images With High-Density Impulsive Noise Based on Sparse Approximation and Ant-Colony Optimization

SHIH-CHIA HUANG¹, (Senior Member, IEEE), YAN-TSUNG PENG², (Member, IEEE),
CHIA-HAO CHANG¹, KAI-HAN CHENG², SHA-WO HUANG²,
AND BO-HAO CHEN³, (Member, IEEE)

¹Department of Electronic Engineering, National Taipei University of Technology, Taipei 10608, Taiwan

²Pervasive Artificial Intelligence Research (PAIR) Labs, Department of Computer Science, National Chengchi University, Taipei 116302, Taiwan

³Department of Computer Science and Engineering, Yuan Ze University, Taoyuan 32003, Taiwan

Corresponding author: Yan-Tsung Peng (ytpeng@cs.nccu.edu.tw)

This work was supported in part by the Ministry of Science and Technology of Taiwan (MOST) under Grant MOST 109-2622-E-027-006-CC3, Grant MOST 108-2221-E-027-047-MY3, Grant MOST 106-2221-E-027-017-MY3, Grant MOST 108-2638-E-002-002-MY2, Grant MOST 108-2218-E-009-056, in part by the MOST Artificial Intelligence Biomedical Research Center, National Cheng Kung University (NCKU), under Grant MOST 109-2634-F-019-001, and in part by the Pervasive Artificial Intelligence Research (PAIR) Labs under Grant MOST 109-2634-F-004-001.

ABSTRACT In this work, we propose an image denoising approach, specifically for “salt-and-pepper noise,” based on the optimized sparse approximation for restoring images contaminated by high-density impulse noise. The proposed method first uses the inverse-distance weighting-based prediction to estimate noise-recovered pixels. It then utilizes DCT-based sparse approximation to further refine the denoised results with the ant colony optimization. Experiments on an image benchmark dataset demonstrate that the proposed method yields better results compared to the state-of-the-art image noise removal methods.

INDEX TERMS Noise removal, sparse approximation, ant-colony optimization.

I. INTRODUCTION

Image communication and acquisition under unfavorable conditions often cause captured images to corrupt with high-density impulse noise [1]. Such image noise can not only degrade visual quality but negatively affect the performance of various computer-vision applications, such as people-counting, crowd analysis, action recognition, human tracking, and so on [1]. Therefore, developing a robust and effective denoising method is essential. In general, conventional denoising methods for removing impulse noise often use median filtering [2] or average filtering. Toh and Isa [3] developed a noise adaptive fuzzy switching median filter to remove impulse noise from corrupted images, obtaining a denoised image by using fuzzy computation via a weighted smoothing for the original and filtered pixels.

Esakirajan *et al.* proposed to use the mean and median filtering conjunctively deal with the high-density noise of an image. An adaptive weighted mean filter [4] recovers noisy

images with adaptively-sized kernels. Hsieh *et al.* [5] developed a fast median filter using two forms of the filtering window to restore images corrupted with high-density impulse noise. The denoising approaches based on the median filtering can generate decent results as long as acquired images are not heavily contaminated by impulse noise. In other words, these approaches cannot deal with images having high-density impulse noise, especially with the noise level over 50%. Erkan *et al.* [6] proposed to use two-pass median filtering with the selective window size for image noise removal. The approach chooses the window size in the first pass, where it contains at least one non-noise pixel, and then applies median filtering. If there are still noise pixels in the window, median filtering is applied again in the second pass to remove the rest of the noise pixels. The main disadvantage of it is that fake edges often exist in its denoised results.

There has been research done using learning-based techniques for image noise removal recently. In particular, sparse approximation approaches with a dictionary learned to restore images with high-density impulse noise for better results than those of median-filter-based methods.

The associate editor coordinating the review of this manuscript and approving it for publication was Yi Zhang¹.

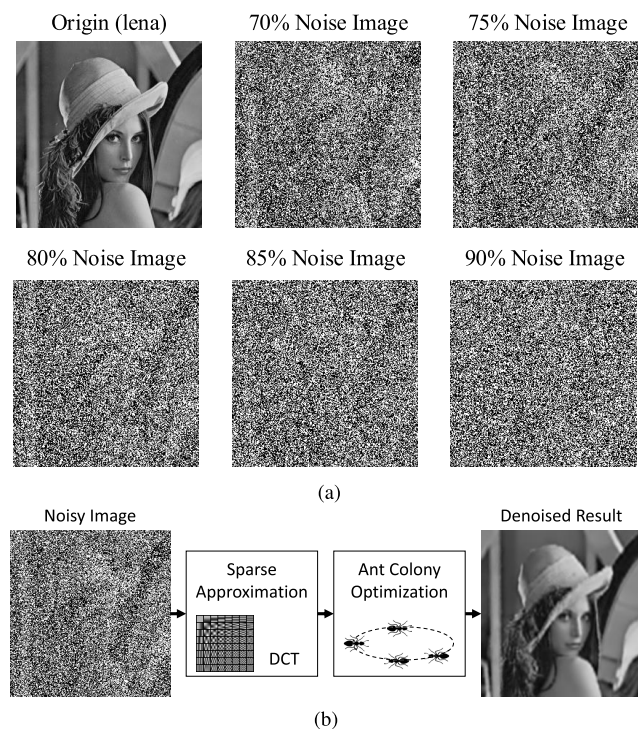


FIGURE 1. (a) Examples of the “Lena” image corrupted with different levels of impulse noise ranging from 70% to 90%. (b) Abstract flowchart for the proposed method.

Chen *et al.* [7] first detected noise candidates via the conjunctive utilization of the adaptive median filter and the adaptive center-weighted median filter, producing denoised images through sparse representation learning from noise-free images. Stanković *et al.* [8], [9] proposed to deal with images taken in impulsive disturbance environments using a gradient-based iterative algorithm to locate and then remove noise pixels. Peng *et al.* [10] proposed an overlapped and adaptive Gaussian smoothing method with convolutional refinement networks for denoising. Liu *et al.* [11] proposed a feature extraction algorithm based on sparse and low-rank representation. Ma *et al.* [12] extended it to get better denoising results by utilizing the total variation regularization based on the sparse representation prior. Jiang *et al.* [13] developed an approach that uses weighted encoding with sparse non-local regularization for high-density impulse noise removal, in which soft impulse pixel detection is applied through weighted encoding to deal with impulse noise. Aggarwal and Majumdar [14] regarded image denoising as a data fidelity minimization problem with l_1 -norm regularization. They then used a split Bregman-based algorithm to solve the problem via the general analysis prior.

Zhang *et al.* [15] proposed feed-forward denoising convolutional neural networks (DnCNNs) that use residual connections and batch normalization to try to deal with more general image denoising tasks at different scales. However, it is often too general to work well on more specific image noise. One common disadvantage these learning-based

methods have is that they often fail to recover images having a high percentage of noise pixels. For example, they usually cannot handle images with a noise level exceeding 70% (see Fig. 1 (a)). It could introduce excessive artifacts in denoised results. In such cases, there are too few noise-free pixels available in the image to sufficiently facilitate the sparse representation based on learning-based techniques.

To address this issue, we propose an effective sparse approximation method based on a DCT dictionary with the ant colony optimization for high-density impulse noise removal. The proposed method consists of two primary modules: a Sparse Representation (SR) module and an Ant-colony Optimization (AO) module.

In order to have enough non-noise information for sparse approximation, the proposed method first adopts an inverse-distance weighting-based prediction to recover noise-tainted pixels in the proposed SR module. Next, it seeks a better prediction of noise-recovered pixels based on ant-colony optimization in the proposed AO module. Fig. 1 (b) shows the abstract flowchart for the proposed method. To sum up, the primary contributions of this paper are:

- 1) We propose a novel denoising method through an effective combination of the SR and AO modules to better reconstruct the corrupted images.
- 2) As far as we know, we are the first to adopt ant-colony optimization for further improving the visual quality of denoised results.
- 3) We evaluate our method with numerous experiments and demonstrate that our method outperforms other state-of-the-art methods.

The remainder of this paper is organized as follows. The proposed method is described in detail in Section II. Section III discusses the comparisons between the proposed method and other state-of-the-art learning-based methods. Section IV concludes the paper.

II. PROPOSED DENOISING METHOD

This paper proposes a novel noise removal approach based on sparse approximation using ant-colony optimization to remove high-density impulse noise from a corrupted image and then recover the image. As illustrated in Fig. 2, our approach consists of two major modules: a sparse representation module and an ant-colony optimization module.

Since noise-free pixels in the input image with high-density noise are not enough for general learning-based denoising methods to learn sparse representations, these methods often fail to reconstruct the de-noised image effectively because of insufficient training patterns. To overcome this problem, the proposed SR module employs the inverse-distance weighting based prediction model to estimate noise-fixed pixels, which serve as non-noise information for learning sparse approximation. Note that the sparse representation module was primarily presented in our previous work [16].

Based on the inverse-distance weighting-based prediction model [17], different sampled noise-free pixels may have different weights for estimating recovered noise pixels. Thus, to

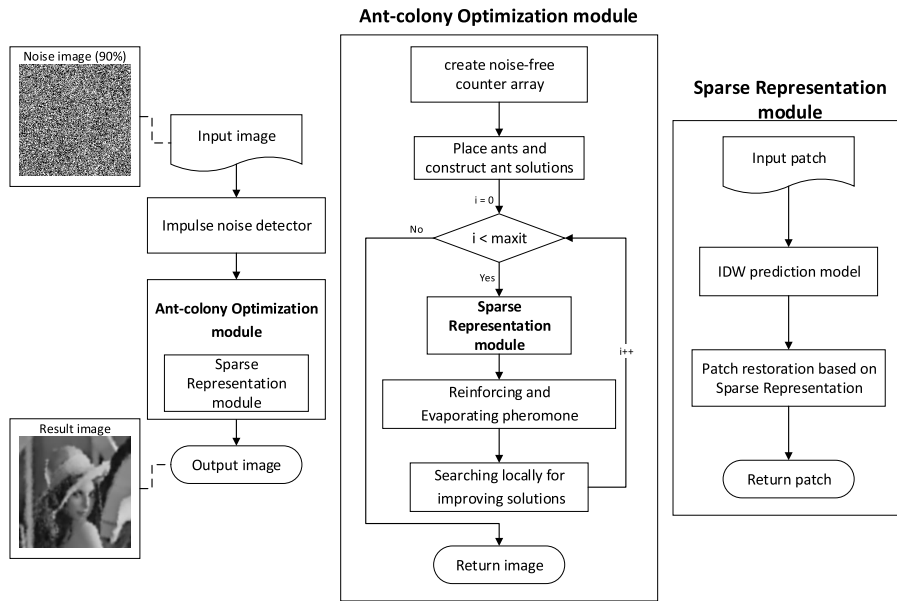


FIGURE 2. Overview of the proposed sparse approximation approach using ant colony optimization.

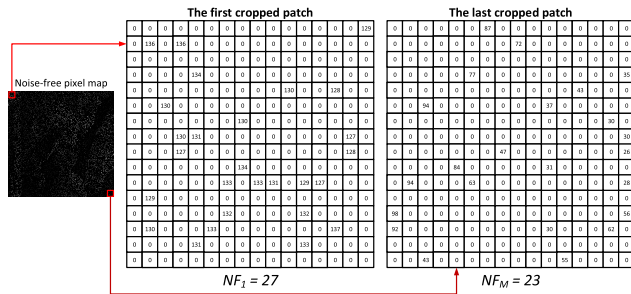


FIGURE 3. Illustration of the noise-free pixel counters NF_i of overlapped image patches. Note that the noise-free pixel map shows all the non-noise pixels as they are in the image whereas setting the noise pixels to 0.

seek a better reconstruction for a de-noised image, ant-colony optimization is used in the proposed AO module.

Initially, the impulse noise detector [18]–[20] is adopted to discriminate noise pixels and noise-free pixels in an image. The impulse noise detector can be expressed as follows:

$$B(x) = \begin{cases} 1, & \text{if } I(x) \text{ is noise;} \\ 0, & \text{otherwise,} \end{cases} \quad (1)$$

where $I(x)$ denotes the intensity value of a pixel at position x , and $B(x)$ denotes the binary noise mask. If the mask is labeled '1', it indicates that the corresponding pixel is either the maximal or minimal intensity values (i.e., 0 or 255 for an 8-bit image). The label '0' represents that the pixel is a noise-free pixel. The detailed description of these two modules is given in the following subsections.

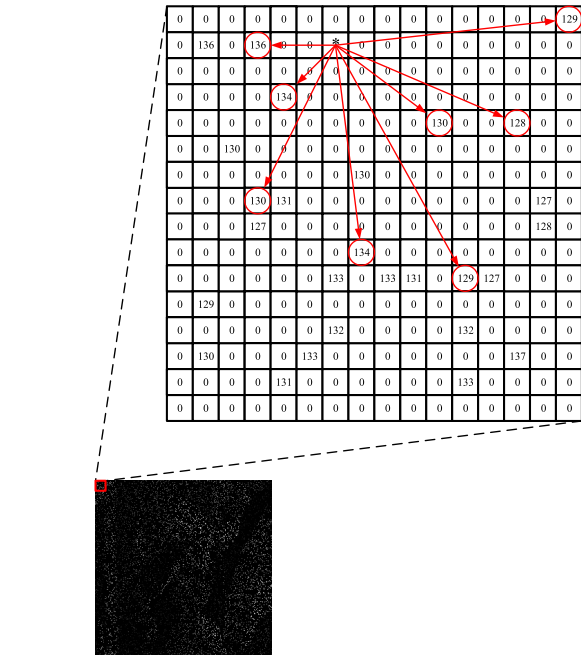


FIGURE 4. Illustration of the distance between the noise pixel (indicated by *) and its surrounding noise-free pixels (marked in red circles) in the inverse-distance weighting-based prediction model.

A. SPARSE REPRESENTATION MODULE

First of all, we decompose the input image I into overlapped patches with size $\sqrt{n} \times \sqrt{n}$, where n is the width of the input square image I . As demonstrated in Fig. 3, we introduce a noise-free pixel counter NF_i for the i th patch, where we use the counter to record the number of noise-free pixels. It can

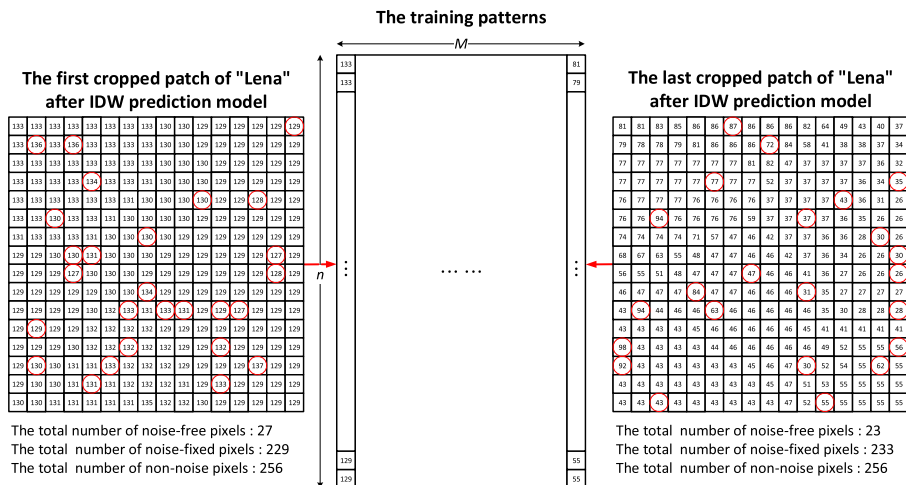


FIGURE 5. Illustration of training patterns based on the IDW prediction results in the proposed SR module. The noise-free pixels are circled in red. The others are the recovered noise pixels in the patch.

be expressed as follows:

$$NF_i = n - \sum_{\forall x \in \Omega(i)} B(x), \quad (2)$$

where $\Omega(i)$ denotes the coordinate set for the pixels in the i_{th} patch.

The minimal value of NF_{min} over overlapped image patches is used as the number of sampled pixels to predict potential noise-fixed pixels in the proposed inverse-distance weighting-based (IDW) prediction model [17]. Note that the number of noise-free pixels might be greater than or equal to the number of sampled pixels. Thus, the inverse-distance weighting based prediction model can be expressed as follows:

$$V(x) = \sum_{i=0}^{NF_{min}} \frac{w_i(x)I(x)}{w_i^{sum}}, \quad s.t. \forall B(x) = 0, \quad (3)$$

where

$$w_i(x) = \frac{1}{d^p}, \quad (4)$$

and $V(x)$ represents the predicted intensity of a potential noise-fixed pixel at position x within the i_{th} overlapped image patch which is interpolated with a set of given intensity of noise-free pixels $I(x)$, $s.t. \forall B(x) = 0$; d is the Euclidean distance between the noise pixel (i.e., $I(x)$, $s.t. \forall B(x) = 1$) and the noise-free pixel (i.e., $I(x)$, $s.t. \forall B(x) = 0$ [See Fig. 4]); w_i^{sum} is the sum of weights within the i_{th} overlapped image patch; p is a predefined power factor. Here, we empirically set $p = 11$ in our experiment.

According to the sparsity-based regularization principle, each overlapped image patch can be sparsely represented as $I_i \approx \phi\alpha_{i,i}$ by solving the following l_1 -minimization problem using the DCT-based dictionary $\phi \in \mathbb{R}^{n \times M}$, $s.t. n \leq M$ [7]:

$$\alpha_{i,i} = \operatorname{argmin}_{\alpha_{i,i}} \left\{ \|I_i - \phi\alpha_{i,i}\|_2^2 + \|\alpha_{i,i}\|_1 \right\}, \quad (5)$$

where $\|I_i - \phi\alpha_{i,i}\|_2^2$ and $\|\alpha_{i,i}\|_1$ are the data-fidelity term and the sparse regularization term, respectively. Next, we can reconstruct a de-noised image from the set of sparse codes $\{\alpha_{i,i}\}$ by using the least-square solution [21] as follows:

$$I \approx \phi \circ \alpha_I = \left(\sum_{i=1}^M R_i^T R_i \right)^{-1} \sum_{i=1}^M R_i^T \phi \alpha_{i,i}, \quad (6)$$

where M is the total number of overlapped patches with size $\sqrt{n} \times \sqrt{n}$ in the image I . Here, in order to reconstruct a de-noised patch, the predicted noise-fixed pixels within the i_{th} overlapped image patch are regarded as the measured patch by which to provide a sufficient training pattern for sparse approximation (See Fig. 5). Therefore, we reformulate the minimization task in Eq. (5) into:

$$\alpha_{i,i} = \operatorname{argmin}_{\alpha_{i,i}} \left\{ \lambda \sum_{i \in \Omega} \|\alpha_{i,i}\|_1 \right\} \quad s.t. \sum_{i \in \Omega} \|I_i - \phi\alpha_{i,i}\|_2^2 \leq \epsilon, \quad (7)$$

where the term $\|I_i - \phi\alpha_{i,i}\|_2^2$ denotes each patch-error with a predefined tolerance ϵ . Note that the i_{th} overlapped image patch I_i is composed of both noise-free pixels and predicted noise-fixed pixels. The error-constrained orthogonal matching pursuit is employed in the proposed SR module for solving the above minimization task [22].

B. ANT-COLONY OPTIMIZATION MODULE

Ant-colony optimization was first introduced in [23] and is regarded as an adaptive meta-heuristic optimization method inspired by nature for solving the combinatorial optimization problems [24]. The principles of ant colony optimization include:

- 1) constructing ant solutions that can balance pheromone trails (i.e., characteristics of past solutions, with a problem-specific heuristic);

- 2) reinforcing and evaporating pheromone;
- 3) searching locally for improved solutions.

The key steps of the proposed ant-colony optimization are described below.

Step 1) Constructing ant solutions: In general, there is a set of solutions $S = \{S_1, \dots, S_l, \dots, S_k\}$ (also called trails) that can satisfy all the constraints in the set, in which each decision variable has a series of values assigned by $s_1^1, \dots, s_l^1, \dots, s_k^M$. Moreover, the solution is feasible for the given optimization problem. The set of solutions is randomly initialized while the series of values in s_i^l is restricted to $0 \leq s_i^l < n \wedge \forall B_i(x) = 0$ for each solution. Therefore, a complete ant solution is composed of an integer vector of size $k \times M$.

Step 2) Reinforcing and evaporating pheromones: After the set of solution is generated, each series of values in s_i^l can be used to reconstruct an overlapped image patch in the proposed SR module. The quality of each solution (i.e., the de-noised image) is evaluated by using the no-reference Q metric. This no-reference metric can be expressed as follows:

$$Q = z_1 \frac{z_1 - z_2}{z_1 + z_2}, \tag{8}$$

where z_1 and z_2 denote the singular values representing the energy observed in the dominant direction V_1 and the perpendicular direction V_2 , respectively. These directions can be obtained as follows:

$$G = USV^* = U \begin{bmatrix} z_1 & 0 \\ 0 & z_2 \end{bmatrix} [V_1 \ V_2]^*, \tag{9}$$

where G denotes the gradient matrix over a local window of size $\sqrt{n} \times \sqrt{n}$. Hence, the dominant orientation of the local window can be obtained by computing the SVD of G [25]. Scores attained by the aforementioned Q metric with higher values indicate superior noise removal effects.

Next, each pheromone is reinforced and evaporated in order to facilitate the construction of a better trail (i.e., solution) that is likely to be feasible and observe the weight and cost constraints. The better trail S_l possesses a higher weight ω ranked by Q and labeled by $l = \{1, \dots, k\}$. The weight ω can be calculated by

$$\omega_l = \frac{1}{qk\sqrt{2\pi}} e^{-\frac{(l-1)^2}{2q^2k^2}}, \tag{10}$$

where k is the number of solution in a set, and q is a tolerance factor that is set to 0.5 in our experiments. Therefore, the new trail is represented by

$$s_{k'}^i = \begin{cases} s_{\text{cdf}(\text{rand}(0,1))}^i, & \text{if } \text{rand}(0,1) > \delta \\ \text{new ant solutions,} & \text{otherwise,} \end{cases} \tag{11}$$

where δ is the mutation factor. If the random value of $\text{rand}(0,1)$ exceeds the mutation factor δ , then the trail is randomly updated by previous trail $s_{\text{cdf}(\text{rand}(0,1))}^i$, where the $\text{cdf}(\cdot)$ denotes the cumulative probability density of weight ω . Otherwise, we create a new solution via Step 1.

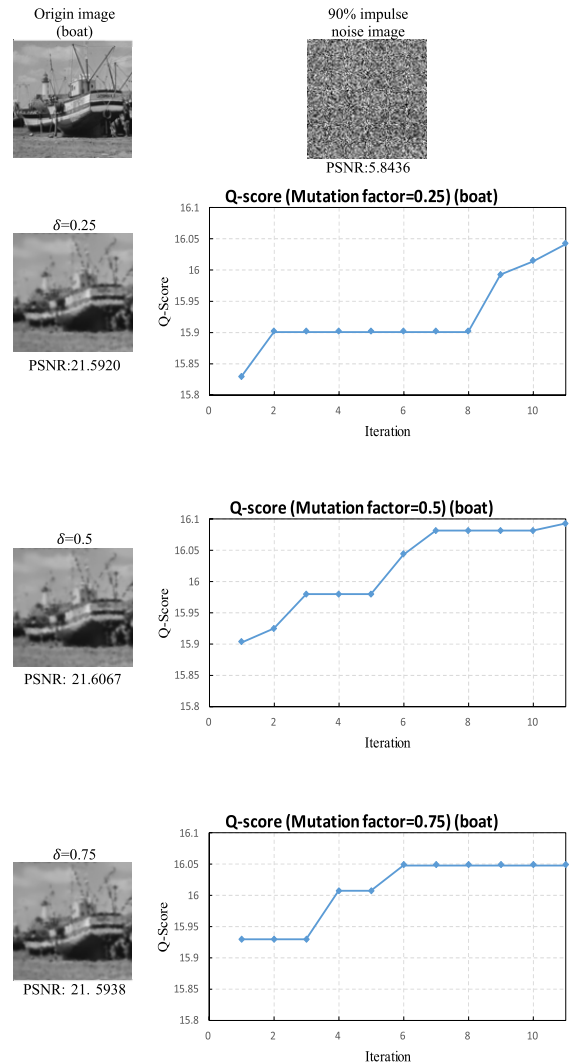


FIGURE 6. Comparison between the reconstructed images via different values of the mutation factor in the proposed AO module.

The lower mutation factor δ possesses higher Q score climbing in order to overcome the local optimum problem [26], as indicated in Fig. 6.

Step 3) Searching locally for improved solutions: Finally, a selection process is performed from the solution set (see Fig. 7) for the next generation. In the solution set S , the solutions assigned with the top ten lowest labels $l = \{1, \dots, k\}$ are maintained into the next generation. By executing the above steps iteratively, the best solutions can be preserved from generation to generation. Therefore, the proposed method is able to effectively remove impulse noise from corrupted images for each level of high-density noise, as shown in Fig. 8.

III. EXPERIMENTAL RESULTS

In this section, the experimental results for high-density impulse noise removal using the proposed approach and three other state-of-the-art approaches are conducted for

S_1	S_1^1	S_1^2	\dots	S_1^i	\dots	S_1^M	$Q(S_1)$	ω_1
S_2	S_2^1	S_2^2	\dots	S_2^i	\dots	S_2^M	$Q(S_2)$	ω_2
\vdots	\vdots	\vdots	\vdots	\vdots	\vdots	\vdots	\vdots	\vdots
S_l	S_l^1	S_l^2	\dots	S_l^i	\dots	S_l^M	$Q(S_l)$	ω_l
\vdots	\vdots	\vdots	\vdots	\vdots	\vdots	\vdots	\vdots	\vdots
S_k	S_k^1	S_k^2	\dots	S_k^i	\dots	S_k^M	$Q(S_k)$	ω_k

FIGURE 7. Illustration of solution set kept by the proposed AO module, in which the solutions are ordered by labels $l = \{1, \dots, k\}$ according to their Q scores for a noise removal problem.

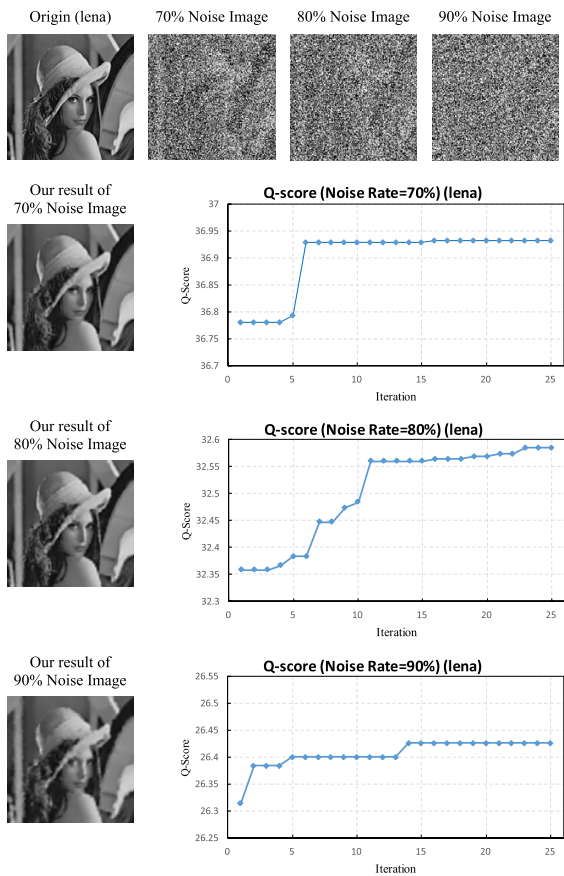


FIGURE 8. Convergence profile of the proposed approach based on sparse approximation using ant colony optimization for removing high-density impulsive noise from the image "Lena," where the percentage of noise ranges from 70% to 90%.

several images corrupted by high-density impulsive noise. These state-of-the-art approaches include Aggarwal *et al.*'s approach [14], Ma *et al.*'s approach [12], and Jiang *et al.*'s approach [13], Erkan *et al.*'s approach [6], and Zhang *et al.*'s approach [15].

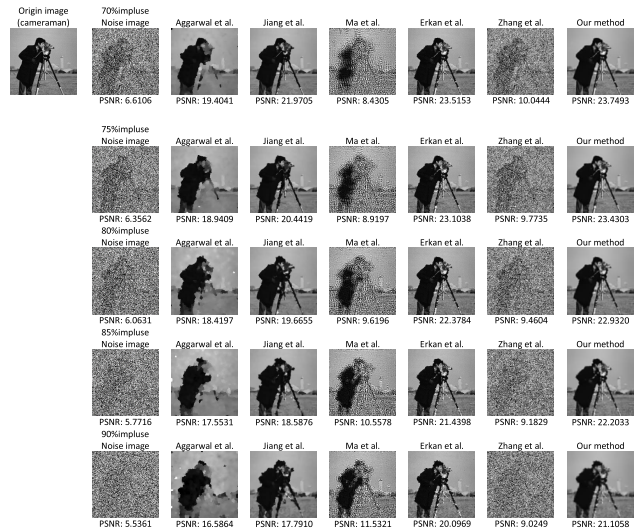


FIGURE 9. Illustration of "Cameraman" image reconstructed via each compared method as impulse noise increases from 70% to 90%.

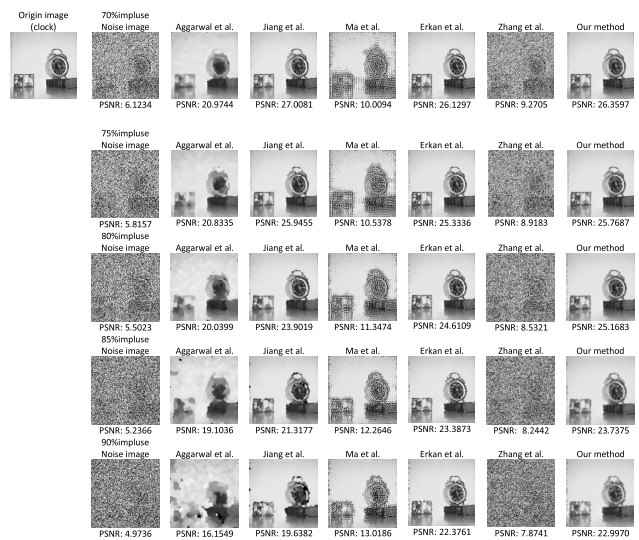


FIGURE 10. Illustration of "Clock" image reconstructed via each compared method as impulse noise increases from 70% to 90%.

A. QUALITATIVE EVALUATION

As can be seen in Figs. 9-14, we visually demonstrate the reconstruction efficacy of each compared method through eight different images corrupted with high-density impulsive noise levels ranging from 70% to 90%. Additionally, we include the corresponding peak signal-to-noise ratio (PSNR) of each reconstruction result.

As can be seen in the third to fifth columns of Figs. 9-14, the reconstructed images obtained through the approaches of Aggarwal and Majumdar [14], Ma *et al.* [12], and Jiang *et al.* [13] appear blurrier and with more serious artifacts compared to the results produced through the proposed method. Aggarwal *et al.*'s approach [14] considered the impulsive noise removal problem as an l_1 -norm regularized

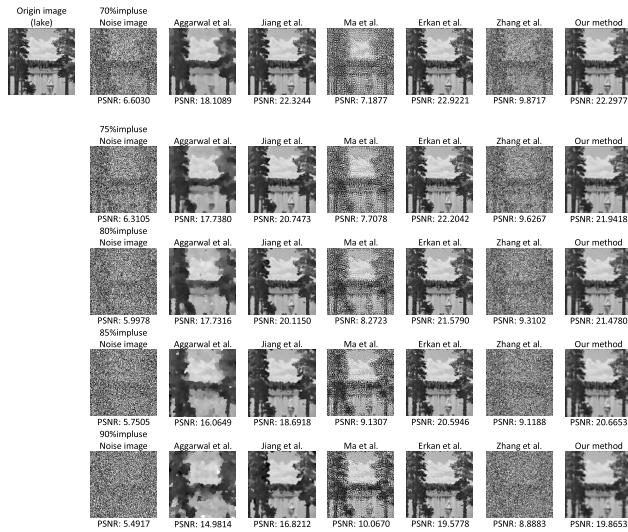


FIGURE 11. Illustration of “Lake” image reconstructed via each compared method as impulse noise increases from 70% to 90%.



FIGURE 12. Illustration of “Lena” image reconstructed via each compared method as impulse noise increases from 70% to 90%.

l_1 -norm data fidelity minimization problem and thereby a noise-free image was produced by solving this problem via a general analysis prior using a split Bregman-based algorithm. Ma *et al.*'s approach [12] conjunctly utilized the sparse representation prior and total variation regularization to seek better recovery results. Jiang *et al.*'s approach [13] employed weighted encoding with sparse nonlocal regularization for high-density impulse noise removal, in which soft impulse pixel detection is employed via weighted encoding to deal with the impulse noise. Additionally, both the image sparsity prior and nonlocal self-similarity prior are used to represent the noise-free image. However, these methods employ insufficient noise-free information with which to predict the unknown corrupted patches for learning sparse approximation when the impulse noise in the corrupted image

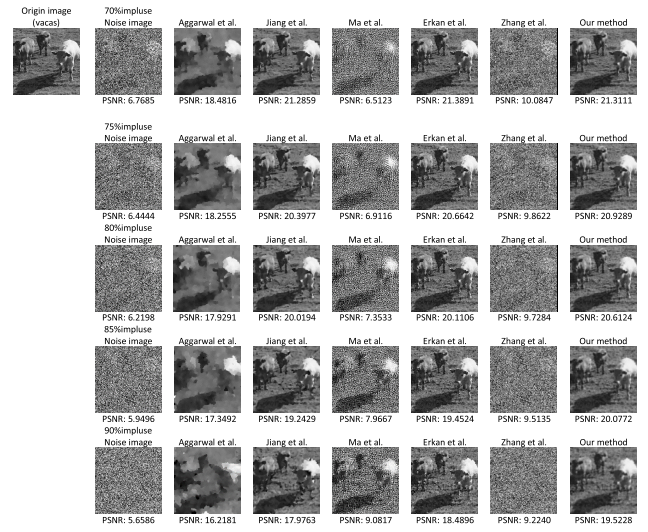


FIGURE 13. Illustration of “Vacas” image reconstructed via each compared method as impulse noise increases from 70% to 90%.

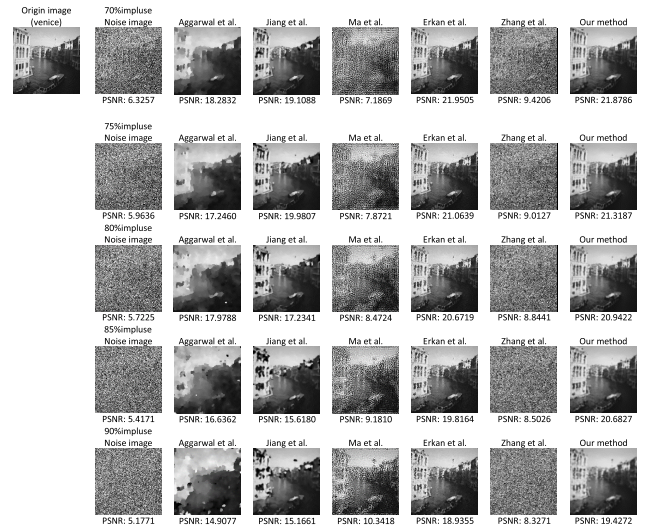


FIGURE 14. Illustration of “Venice” image reconstructed via each compared method as impulse noise increases from 70% to 90%.

exceeds 70%. Erkan *et al.*'s approach [6] produces relatively clear results but introduces more false edges and artifacts. Zhang *et al.*'s approach [15] does not work at all for images with impulsive noise.

As can be observed in the sixth column of Figs. 9-14, our approach is capable of yielding clearer results than the other state-of-the-art approaches, and those results possess higher PSNR scores. This is because the proposed SR module employs an inverse-distance weighting-based prediction model to produce potential noise-fixed pixels by which to sufficiently provide non-noise pixels for sparse approximation. Additionally, ant-colony optimization is used with the no-reference Q metric in the proposed AO module to seek an optimized prediction of a de-noised image. As such, the PSNR scores in Figs. 9-14 demonstrate that the corrupted

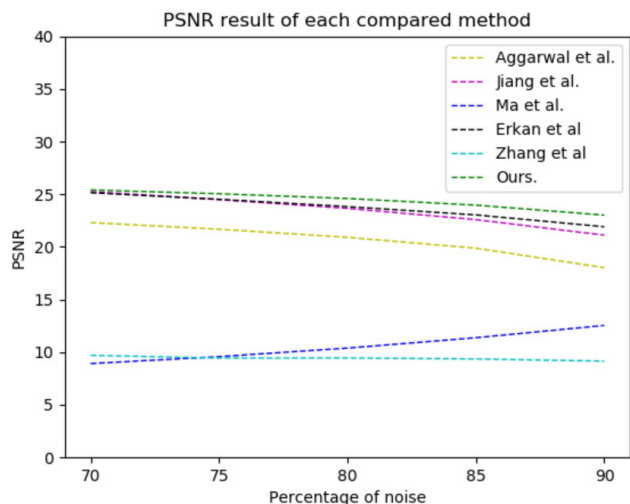


FIGURE 15. Comparison of PSNR results between each compared method for fifteen high-density noise images, where the percentage of noise ranges from 70% to 90%.



FIGURE 16. All the images in our test dataset.

images are recovered more effectively through our approach than through the others.

B. QUANTITATIVE EVALUATION

Next, the quantitative results obtained by the proposed approach are compared with those obtained by the approaches of Aggarwal and Majumdar [14], Ma et al. [12], Jiang et al. [13], Erkan et al. [6], and Zhang et al. [15], in terms of the average PSNR [27] over 70 gray scale image sets. Note that higher rates produced by the PSNR metric indicate superior noise removal effects.

As shown in Fig. 15, the PSNR scores of images reconstructed via the approaches of Aggarwal and Majumdar [14], Jiang et al. [13], and Erkan et al. [6] indicate those reconstructions degrade as the impulse noises increased. Regarding the

approach of Ma et al. [12], while the PSNR score increases for its reconstructed images, they inevitably suffered from artifacts, and the PSNR is still lower than that of the other compared approaches. The PSNR score of Zhang et al.'s approach [15] shows that it cannot deal with images with such noise at all. The PSNR scores for the images reconstructed by our method did not degrade as much as noise increased, and thus outperformed the results from the approaches of Aggarwal and Majumdar [14], Ma et al. [12], Jiang et al. [13], Erkan et al. [6], and Zhang et al. [15]. The results also show that the proposed method is capable of performing superior noise removal while recovering texture information effectively.

IV. CONCLUSIONS

This paper has presented a new de-noising method based on optimized sparse approximation using ant-colony optimization for high-density impulse noise removal from a corrupted image. The proposed method allows high-density impulse noise removal from corrupted images, which is strongly required in several computer-vision systems. Unlike existing methods that use the corrupted texture information or remnant noise-free information to reconstruct a de-noised image, our method employs the inverse-distance weighting based prediction model to produce potential noise-fixed pixels for sparse approximation learning. This gives the proposed method the ability to remove high-density impulse noise from the corrupted image. Additionally, the proposed method adopt the ant-colony optimization to seek an optimized non-noise image reconstruction, in which the no-reference Q metric is used to evaluate the reconstructed image at each generation for improving the quality of the reconstruction result in accordance with its original value. A comprehensive evaluation of the results produced by the different compared methods via qualitative and quantitative assessments for image noise removal is conducted in this paper. Our experimental results, using various test images with varying levels of high-density noise and comparing the results through different evaluations, demonstrate the effectiveness of the proposed method, its ability to outperform the other state-of-the-art sparse approximation approaches, and its robustness for high-density impulse noise removal.

REFERENCES

- [1] S.-C. Huang, "An advanced motion detection algorithm with video quality analysis for video surveillance systems," *IEEE Trans. Circuits Syst. Video Technol.*, vol. 21, no. 1, pp. 1–14, Jan. 2011.
- [2] T. Nodes and N. Gallagher, "Median filters: Some modifications and their properties," *IEEE Trans. Acoust., Speech, Signal Process.*, vol. 30, no. 5, pp. 739–746, Oct. 1982.
- [3] K. K. V. Toh and N. A. M. Isa, "Noise adaptive fuzzy switching median filter for salt-and-pepper noise reduction," *IEEE Signal Process. Lett.*, vol. 17, no. 3, pp. 281–284, Mar. 2010.
- [4] P. Zhang and F. Li, "A new adaptive weighted mean filter for removing Salt-and-Pepper noise," *IEEE Signal Process. Lett.*, vol. 21, no. 10, pp. 1280–1283, Oct. 2014.
- [5] M.-H. Hsieh, F.-C. Cheng, M.-C. Shie, and S.-J. Ruan, "Fast and efficient median filter for removing 1–99% levels of salt-and-pepper noise in images," *Eng. Appl. Artif. Intell.*, vol. 26, no. 4, pp. 1333–1338, Apr. 2013, doi: 10.1016/j.engappai.2012.10.012.

- [6] U. Erkan, L. Gökrem, and S. Enginoğlu, "Different applied median filter in salt and pepper noise," *Comput. Electr. Eng.*, vol. 70, pp. 789–798, Aug. 2018.
- [7] F. Chen, G. Ma, L. Lin, and Q. Qin, "Impulsive noise removal via sparse representation," *J. Electron. Imag.*, vol. 22, no. 4, 2013, Art. no. 043014, doi: 10.1117/1.JEI.22.4.043014.
- [8] I. Stanković, I. Orović, M. Daković, and S. Stanković, "Denoising of sparse images in impulsive disturbance environment," *Multimedia Tools Appl.*, vol. 77, no. 5, pp. 5885–5905, Mar. 2018.
- [9] L. Stanković, M. Daković, and S. Vujović, "Reconstruction of sparse signals in impulsive disturbance environments," *Circuits, Syst., Signal Process.*, vol. 36, no. 2, pp. 767–794, Feb. 2017.
- [10] Y.-T. Peng, M.-H. Lin, C.-L. Tang, and C.-H. Wu, "Image denoising based on overlapped and adaptive Gaussian smoothing and convolutional refinement networks," in *Proc. IEEE Int. Symp. Multimedia (ISM)*, Dec. 2019, pp. 136–1363.
- [11] Z. Liu, W. Ou, W. Lu, and L. Wang, "Discriminative feature extraction based on sparse and low-rank representation," *Neurocomputing*, vol. 362, pp. 129–138, Oct. 2019.
- [12] L. Ma, J. Yu, and T. Zeng, "Sparse representation prior and total variation-based image deblurring under impulse noise," *SIAM J. Imag. Sci.*, vol. 6, no. 4, pp. 2258–2284, Jan. 2013, doi: 10.1137/120866452.
- [13] J. Jiang, L. Zhang, and J. Yang, "Mixed noise removal by weighted encoding with sparse nonlocal regularization," *IEEE Trans. Image Process.*, vol. 23, no. 6, pp. 2651–2662, Jun. 2014.
- [14] H. K. Aggarwal and A. Majumdar, "Exploiting spatio-spectral correlation for impulse denoising in hyperspectral images," *J. Electron. Imag.*, vol. 24, no. 1, Feb. 2015, Art. no. 013027, doi: 10.1117/1.JEI.24.1.013027.
- [15] K. Zhang, W. Zuo, Y. Chen, D. Meng, and L. Zhang, "Beyond a Gaussian denoiser: Residual learning of deep CNN for image denoising," *IEEE Trans. Image Process.*, vol. 26, no. 7, pp. 3142–3155, Jul. 2017.
- [16] B. H. Chen, C. H. Chang, and S. C. Huang, "Denoising using inverse-distance weighting with sparse approximation," in *Proc. IEEE Int. Symp. Multimedia (ISM)*, Dec. 2016, pp. 439–444.
- [17] G. Y. Lu and D. W. Wong, "An adaptive inverse-distance weighting spatial interpolation technique," *Comput. Geosci.*, vol. 34, no. 9, pp. 1044–1055, Sep. 2008. [Online]. Available: <http://www.sciencedirect.com/science/article/pii/S0098300408000721>
- [18] I. Aizenberg and C. Butakoff, "Effective impulse detector based on rank-order criteria," *IEEE Signal Process. Lett.*, vol. 11, no. 3, pp. 363–366, Mar. 2004.
- [19] Y. Dong and S. Xu, "A new directional weighted median filter for removal of random-valued impulse noise," *IEEE Signal Process. Lett.*, vol. 14, no. 3, pp. 193–196, Mar. 2007.
- [20] C.-Y. Lien, C.-C. Huang, P.-Y. Chen, and Y.-F. Lin, "An efficient denoising architecture for removal of impulse noise in images," *IEEE Trans. Comput.*, vol. 62, no. 4, pp. 631–643, Apr. 2013.
- [21] M. Elad and M. Aharon, "Image denoising via sparse and redundant representations over learned dictionaries," *IEEE Trans. Image Process.*, vol. 15, no. 12, pp. 3736–3745, Dec. 2006.
- [22] R. Rubinstein, M. Zibulevsky, and M. Elad, "Efficient implementation of the K-SVD algorithm and the Batch-OMP method," Dept. Comput. Sci., Technion, Haifa, Israel, Tech. Rep. CS-2008-08, 2008.
- [23] M. Dorigo, "Optimization, learning and natural algorithms," Ph.D. dissertation, Dept. Syst. Inf. Eng., Politecnico di Milano, Milan, Italy, 1992.
- [24] K. Socha and M. Dorigo, "Ant colony optimization for continuous domains," *Eur. J. Oper. Res.*, vol. 185, no. 3, pp. 1155–1173, 2008. [Online]. Available: <http://www.sciencedirect.com/science/article/pii/S0377221706006333>
- [25] X. Zhu and P. Milanfar, "Automatic parameter selection for denoising algorithms using a no-reference measure of image content," *IEEE Trans. Image Process.*, vol. 19, no. 12, pp. 3116–3132, Dec. 2010.
- [26] R. SinghJadon and U. Dutta, "Modified ant colony optimization algorithm with uniform mutation using self-adaptive approach," *Int. J. Comput. Appl.*, vol. 74, no. 13, pp. 5–8, Jul. 2013.
- [27] F.-C. Cheng and S.-C. Huang, "Efficient histogram modification using bilateral bezier curve for the contrast enhancement," *J. Display Technol.*, vol. 9, no. 1, pp. 44–50, Jan. 2013.



SHIH-CHIA HUANG (Senior Member, IEEE) received the B.S. degree from National Taiwan Normal University, Taipei, Taiwan, the M.S. degree from National Chiao Tung University, Hsinchu, Taiwan, and the Ph.D. degree in electrical engineering from National Taiwan University, Taipei, in 2009. He is currently a Full Professor with the Department of Electronic Engineering, National Taipei University of Technology, Taipei. He is also an International Adjunct Professor with the Faculty of Business and Information Technology, University of Ontario Institute of Technology, Oshawa, ON, Canada. He has authored or coauthored more than 100 journal articles and conference papers. He holds more than 60 patents in the U.S., Europe, Taiwan, and China. His research interests include intelligent multimedia systems, image processing, video coding, video surveillance systems, cloud computing, big data analytics, artificial intelligence, and mobile applications and systems. He was a recipient of the Kwoh-Ting Li Young Researcher Award, in 2011, by the Taipei Chapter of the Association for Computing Machinery, the 5th National Industrial Innovation Award, in 2017, by the Ministry of Economic Affairs, Taiwan, the Dr. Shechtman Young Researcher Award, in 2012, by the National Taipei University of Technology, the Outstanding Research Award from the National Taipei University of Technology, in 2014 and 2017, and the College of Electrical Engineering and Computer Science, National Taipei University of Technology, from 2014 to 2016. He is also the Services and Applications Track Chair of the IEEE CloudCom 2016–2017 Conference, the Applications Track Chair of the IEEE BigData Congress, in 2015, the General Chair of the 2015–2016 IEEE BigData Taipei Satellite Session, and the Deep Learning, Ubiquitous and Toy Computing Minitrack Chair. He is also the Chapter Chair of the IEEE Taipei Section Broadcast Technology Society. He is also an Associate Editor of the *IEEE SENSORS JOURNAL* and *Electronic Commerce Research and Applications*. He had been an Associate Editor of the *Journal of Artificial Intelligence*. He was a Guest Editor of the *Engineering Applications of Artificial Intelligence*, *Information Systems Frontiers*, and the *International Journal of Web Services Research*.



YAN-TSUNG PENG (Member, IEEE) received the Ph.D. degree in electrical and computer engineering from the University of California at San Diego, San Diego, in 2017. He was a Senior Engineer with Qualcomm Technologies Inc., in 2019. He joined the Department of Computer Science, National Chengchi University, Taipei, Taiwan, where he is currently an Assistant Professor. His research interests include image processing, video compression, and machine learning and its applications.



CHIA-HAO CHANG received the B.S. and M.S. degrees in electronic engineering from the National Taipei University of Technology, Taipei, in 2014 and 2016, respectively. His research interests include digital image processing and optimization problems.



KAI-HAN CHENG is currently pursuing the M.S. degree with the Department of Computer Science, National Chengchi University. His research interests include image processing and deep learning.



SHA-WO HUANG is currently pursuing the M.S. degree with the Department of Computer Science, National Chengchi University. Her research interests include image processing and deep learning.



BO-HAO CHEN (Member, IEEE) received the Ph.D. degree in electronic engineering from the National Taipei University of Technology, Taipei, Taiwan, in 2014. He is currently an Associate Professor with the Department of Computer Science and Engineering, Yuan Ze University, Taoyuan, Taiwan. His current research interests include computer vision, closely integrated with deep learning, autonomous vehicles, knowledge representation/reasoning, and human-computer interaction. He was a recipient for involvement in research with the Department of Cybernetics, Tula State University, Tula, Russia, in 2014. He has received the Best Student Paper Award from the IEEE International Symposium on Multimedia, in 2013, the Best Paper Award from the ACM International Conference on Big Data and Advanced Wireless Technologies, in 2016, the First Paper Award from the IEEE International Conference on Applied System Innovation, in 2017, the Young Scholar Research Award from the Yuan Ze University, in 2017, and the Best Ph.D. Dissertation Award from the IEEE Taipei Section and the Taiwan Institute of Electrical and Electronic Engineering, in 2014. Since 2020, he has been a Guest Editor of *MDPI Mathematics*.

...